

# Effect of Channel Orientation and Rib Pitch-to-Height Ratio on Pressure Drop in a Rotating Square Channel with Ribs on Two Opposite Surfaces

**S. V. Prabhu**

*Department of Mechanical Engineering, Indian Institute of Technology, Bombay, Powai, Mumbai-400 076, India  
Email: svprabhu@me.iitb.ac.in*

**Neelabh Arora**

*Department of Mechanical Engineering, Indian Institute of Technology, Bombay, Powai, Mumbai-400 076, India  
Email: neelabh@me.iitb.ac.in*

**R. P. Vedula**

*Department of Mechanical Engineering, Indian Institute of Technology, Bombay, Powai, Mumbai-400 076, India  
Email: rpv@me.iitb.ac.in*

*Received 29 September 2003*

The effect of channel orientation and rib pitch-to-height ratio on the pressure drop distribution in a rib-roughened channel is an important issue in turbine blade cooling. The present investigation is a study of the overall pressure drop distribution in a square cross-sectioned channel, with rib turbulators, rotating about an axis normal to the free stream. The ribs are configured in a symmetric arrangement on two opposite surfaces with a rib angle of  $90^\circ$  to the mainstream flow. The study has been conducted for three Reynolds numbers, namely, 13 000, 17 000, and 22 000 with the rotation number varying from 0–0.38. Experiments have been carried out for various rib pitch-to-height ratios ( $P/e$ ) with a constant rib height-to-hydraulic diameter ratio ( $e/D$ ) of 0.1. The test section in which the ribs are placed on the leading and trailing surfaces is considered as the base case (orientation angle =  $0^\circ$ , Coriolis force vector normal to the ribbed surfaces). The channel is turned about its axis in steps of  $15^\circ$  to vary the orientation angle from  $0^\circ$  to  $90^\circ$ . The overall pressure drop does not change considerably under conditions of rotation for the base case. However, for the other cases tested, it is observed that the overall pressure drop increases with an increase in the rotation number for a given orientation angle and also increases with an increase in the orientation angle for a given rotation number. This change is attributed to the variation in the separation zone downstream of the ribs due to the presence of the Coriolis force—local pressure drop data is presented which supports this idea. At an orientation angle of  $90^\circ$  (ribs on the top and bottom surfaces, Coriolis force vector normal to the smooth surfaces), the overall pressure drop is observed to be maximum during rotation. The overall pressure drop for a case with a rib pitch-to-height ratio of 5 on both surfaces is found to be the highest among all the rib pitch-to-height ratios covered in this study with the maximum increase in the overall pressure drop being as high as five times the corresponding no-rotation case at the highest rotation number of 0.38 and  $90^\circ$  orientation angle.

**Keywords and phrases:** rotation, ribs, turbine blade cooling, orientation, pressure drop.

## 1. INTRODUCTION

Convection cooling is one of the cooling mechanisms employed in advanced gas turbine designs in order to increase inlet pressures and temperatures so as to achieve high thrust/weight ratios and low specific fuel consumption. Heat

transfer enhancement is required on the pressure and suction surfaces of the cooling passages in order to transfer more heat from airfoil external surfaces which are directly exposed to the hot gas flow. Turbulence promoters (i.e., repeated ribs with an appropriate rib angle) are often cast onto the two opposite surfaces of the internal passages experiencing the hot mainstream gases for heat transfer enhancement. A typical cooling passage can be modeled as a straight or a multipass square channel with two opposite rib-roughened surfaces.

Geometric parameters such as rib height-to-hydraulic diameter ratio ( $e/D$ ), rib pitch-to-height ratio ( $P/e$ ), the rib angle, the manner in which the ribs on opposite walls are positioned relative to one another (in-line, staggered, criss-cross, etc.) have pronounced effects on both the pressure drop and heat transfer characteristics. Some of these effects have been studied by several investigators. Han et al. [1] studied the effect of rib pitch-to-height ratios (10 and 20) for rib angles of  $30^\circ$ ,  $45^\circ$ ,  $60^\circ$ , and  $90^\circ$  on the pressure drop and the heat transfer distribution in a square duct. They reported that the maximum pressure drops are observed at a rib pitch-to-height ratio of 10 for all rib angles. However, for a rib pitch-to-height ratio of 10, the maximum pressure drop is seen for a rib angle of  $60^\circ$ . Okamoto et al. [2] reported detailed velocity and turbulence intensity measurements over repeated two-dimensional square  $90^\circ$  ribs. They observed that a rib pitch-to-height ratio of 9 is optimum for a highest turbulence intensity and pressure loss. Therefore, a rib pitch-to-height ratio of 10 is often the choice for obtaining high heat transfer coefficients. Three-dimensional velocity measurements of periodic fully developed main and secondary flows in a rectangular channel with rib-roughened surfaces on two opposite sides with an in-line arrangement for a rib pitch-to-height ratio of 10 and a rib height-to-hydraulic diameter ratio of 0.133 were carried out by Liou et al. [3]. They found that the dividing streamline separated the core flow from the main recirculating flow behind the rib and reattached onto the wall at a distance of 3.5 times the rib height. Maximum shear stress and turbulent kinetic energy values were reported to occur slightly upstream of the reattachment point ( $0.6e$ ).

Han and Zhang [4] investigated the combined effects of flow channel aspect ratio, the rib angle, the rib height, and the sharp  $180^\circ$  bend on the distributions of the local pressure drop in a stationary three-pass channel. They reported that a rib angle of  $60^\circ$  yields the highest pressure drop. Taslim and Wadsworth [5] studied the effect of three rib height-to-hydraulic diameter ratios of 0.133, 0.167, and 0.25 for rib pitch-to-height ratios of 5, 8.5, and 10 in a  $90^\circ$  ribbed square channel on the rib heat transfer distribution. A rib pitch-to-height ratio of 8.5 consistently produced the highest rib average heat transfer coefficients.

Rothe and Johnston [6] studied the turbulent separated flow downstream of a backward-facing step in a two-dimensional channel rotating about an axis normal to the free-stream direction. They observed that the free shear layer is stabilized on the suction surface and destabilized on the pressure surface. On the pressure (destablized) surface, increased entrainment tends to increase streamline curvature and reduce the reattachment distance, whereas the reattachment distance increases on the suction surface. This would suggest that the pressure drop characteristics could be different for situations where orthogonal rotation is present. Johnson et al. [7] reported that gas turbine blade internal coolant passages are often oriented at angles that are as large as  $\pm 50^\circ$ – $60^\circ$  to the axis of rotation with the angle varying widely between the mid-chord, leading, and trailing edge regions of the rotating airfoil. The influences of channel orientation

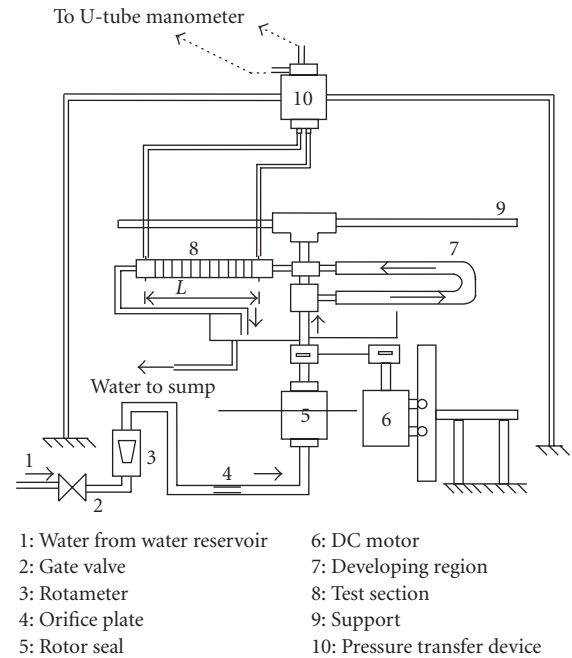


FIGURE 1: Experimental set-up.

on the local heat transfer coefficient in a rotating two-pass square channel with  $60^\circ$  and  $90^\circ$  ribs on the leading and trailing surfaces were investigated by Parsons et al. [8]. The rib height-to-hydraulic diameter ratio of 0.125 and the rib pitch-to-height ratio of 10 were maintained constant. They observed that the effects of the Coriolis force and cross-stream flow reduced as the channel orientation changed from  $0^\circ$  to  $45^\circ$ . Dutta and Han [9] studied heat transfer in a two-pass square channel with rib-roughened surfaces. The ribs were placed in a staggered half-V fashion and experiments were conducted for three orientation angles namely  $0^\circ$ ,  $45^\circ$ , and  $90^\circ$ . They found that staggered half-V ribs show a higher heat transfer coefficient compared to continuous ribs for both  $60^\circ$  and  $90^\circ$  ribs under conditions of rotation.

The literature survey presented above indicates that pressure drop data is not available for varying rib pitch-to-height ratios in the presence of rotation and varying channel orientations. The reported influence of rotation on the separation zone behind a backward facing step suggests that there could be significant differences between the stationary and rotating configurations on the pressure drop in rotating channels with ribs provided for heat transfer enhancement. The objective of this paper is to study the effect of the channel orientation angle and the rib pitch-to-height ratio on the overall pressure drop under conditions of rotation in the presence of ribs on two opposite surfaces. Limited data on the local pressure drop distribution in between the ribs is also presented which aids in explaining the overall pressure drop behaviour.

## 2. EXPERIMENTAL SET-UP

A schematic diagram of the experimental set-up is shown in Figure 1. Water is used as the working fluid and a large

TABLE 1: List of configurations tested.

Case	Rib angle	$P/e$ ratio of the ribs on the leading surface	$P/e$ ratio of the ribs on the trailing surface
$P/e = 3, 3$	$90^\circ$	3	3
$P/e = 5, 5$	$90^\circ$	5	5
$P/e = 10, 10$	$90^\circ$	10	10
$P/e = 10, 5$	$90^\circ$	10	5
$P/e = 10, 8$	$90^\circ$	10	8
$P/e = 15, 5$	$90^\circ$	15	5
$P/e = 10, 10$	$45^\circ$	10	10

rectangular tank of about 2000-litre capacity is used as a reservoir to store water. The tank is placed nearly two meters above the ground level and water is continuously supplied to the tank by a pump from the main supply line. An overflow line connected at the top of the tank ensures a constant level and therefore constant flow rate to the test section. A siphon line from the tank supplies water to the test section through a gate valve, rotameter, and rotor seal. The gate valve upstream of the rotameter is used to set the experimental Reynolds number. An accurately calibrated orifice meter in the line is also used for flowmetering and measurements are almost identical with that of the rotameter. A commercially available rotor seal enables the transfer of water from stationary piping to the rotating test section. A galvanized iron pipe screwed on to the top of the seal has a pulley fit on it by friction which is rotated by a one HP DC motor through a belt-driven pulley and supplies water to the test section through a sufficiently long pipe in order to ensure fully developed flow.

The test section is 0.9 m long with a  $0.03 \text{ m} \times 0.03 \text{ m}$  cross section and is fabricated by chemically bonding machined Plexiglas surfaces. Plexiglas ribs of 0.03 m length with a  $0.003 \times 0.003 \text{ m}$  cross section are glued periodically on the leading and trailing surfaces over a length of 0.35 m in the middle of the test section. The ribs on the two surfaces are symmetric with respect to each other. The rib pitch-to-height ratio ( $P/e$ ) is varied for a constant rib height-to-hydraulic diameter ratio ( $e/D$ ) of 0.1 for two rib angles of  $90^\circ$  and  $45^\circ$ . The details of the various configurations studied are presented in Table 1 shown for the base case.

Orientation angle is the angle obtained by turning the channel about its axis with reference to the base case. Figure 2a shows the definition of the orientation angle. The test section in which the ribs are placed on the leading and trailing surfaces is the base case (orientation angle =  $0^\circ$ ). The direction of the Coriolis force is normal to the leading and trailing surfaces (ribbed walls) and parallel to the top and bottom surfaces for the base case. The Coriolis force is normal to the smooth surfaces and the ribbed walls are the top and bottom surfaces for a channel orientation angle of  $90^\circ$ . The channel is turned about its axis in steps of  $15^\circ$  to obtain the experimental data.

The pressure drop in the rotating test section is measured by a stationary U-tube differential manometer with carbon-tetrachloride as the manometer fluid. The pressure transfer

between the taps on the rotating test section and the stationary manometer was achieved through a specially fabricated pressure transfer device using two commercially available rotor seals. The body force due to the centrifugal force acts both on the fluid within the test section and the manometric limb which is taken from the location of measurement to the axis of rotation. Hence, the measured pressure drop does not include the variation of static pressure due to the difference in the centrifugal force at the two pressure taps. The pressure transfer device was checked for fluid intercommunication between two rotor seals using water at pressures far exceeding those encountered in the present study. Interchanging the connections to the manometer for pressure measurement in the presence of rotation showed no change indicating no bias between the channels of the pressure transfer mechanism. Nonrotating data was also obtained without the device and an accurate match between these measurements and those with the device in the absence of rotation ensured proper working of the device.

The overall mean pressure drop is defined as the calculated difference between the arithmetic average values of pressure drop on all four surfaces (trailing surface, leading surface, top surface, and bottom surface) at the channel entrance and the channel exit of the test section. The resulting average like this or by physically interconnecting the four pressure taps at a given location and then measuring the pressure drop was found to be identical. The overall mean pressure drop is used to calculate the average friction factor given by

$$f = \frac{P_2 - P_1}{(1/2)\rho V^2 (4(L/D))}. \quad (1)$$

$P_1$  and  $P_2$  are the static pressures measured at a distance of 1D upstream of the first rib and 1D downstream of the last rib, respectively, as shown in Figure 2b. The distance “ $L$ ” in the above equation is the distance between the first and the last tap which is 0.41 m in length. The maximum uncertainty in the average friction factor is about 6% by the uncertainty estimation method of Kline and McClintock [10] at a 95% confidence level. The average friction factor is normalized by the friction factor for fully developed turbulent flow in smooth circular tubes proposed by Blasius ( $f(\text{FD}) = 0.046 \text{ Re}^{-0.2}$  for  $10\,000 \leq \text{Re} \leq 100\,000$ ).

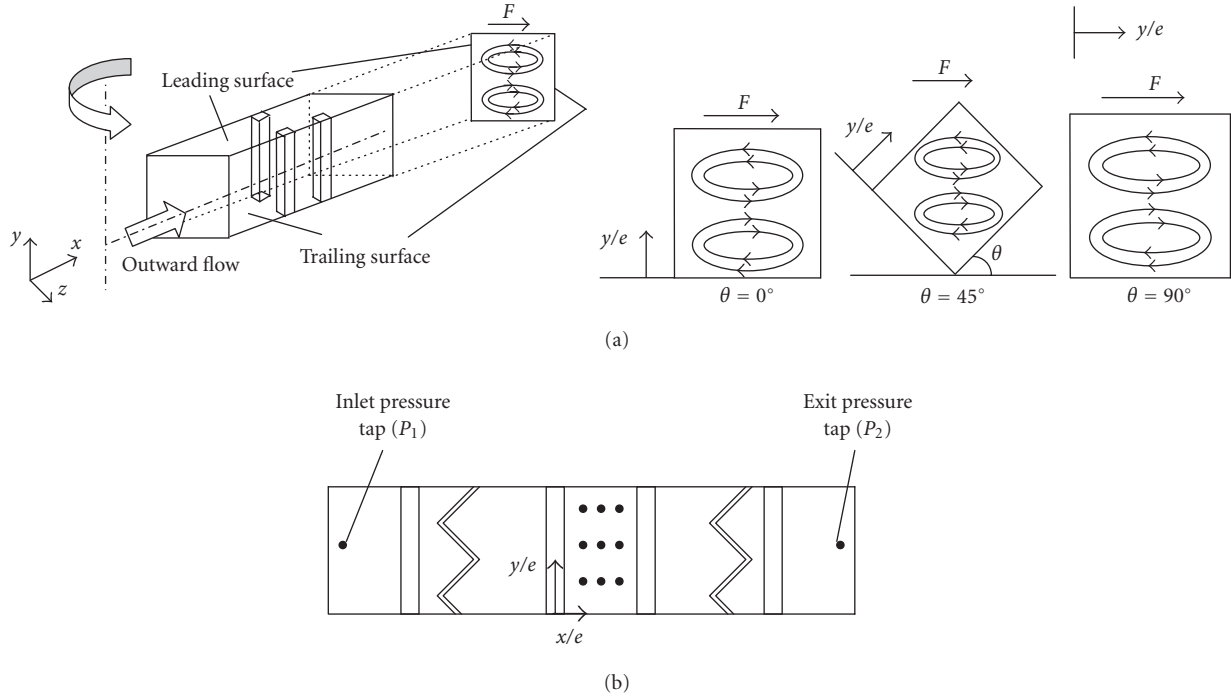


FIGURE 2: (a) Three-dimensional sketch of the test section along with the definition of orientation angle. (b) Sketch showing the static pressure tap locations.

The locations of the pressure taps for the local pressure drop measurements are shown in Figure 2b. Three pressure taps are located at each axial location of  $x/e = 2.5, 5$ , and  $7.5$  for spanwise locations of  $y/e = 2.5, 5$ , and  $7.5$ . These measurements are carried out only for a rib pitch-to-height ratio of 10 and only one wall of the test section had ribs on it. The data is presented as a nondimensional pressure using

$$C_P = \frac{P_{\text{local}} - P_{\text{ref}}}{(1/2)\rho V^2}. \quad (2)$$

$P_{\text{local}}$  is the local pressure at a given location identified by  $x/e$  and  $y/e$  and  $P_{\text{ref}}$  is the reference pressure (arbitrarily chosen to be the pressure at  $x/e = 2.5$  for a given  $y/e$ ).

### 3. RESULTS AND DISCUSSIONS

#### 3.1. Friction factor ratio distribution in a stationary channel for a rib angle of 90°

Water is used as the working medium since very high rotation numbers can be simulated at low rotational speeds. However, the effects of buoyancy cannot be studied. Therefore, in the present case, the friction factor ratio is a function of Reynolds number and rotation number only. Figure 3 shows the friction factor ratio variations for a 90° ribbed channel with a rib height-to-hydraulic diameter ratio of 0.1, and all the rib pitch-to-height ratios ( $P/e$ ) listed in Table 1 are not included in the figure for the sake of clarity. Experiments were conducted for three Reynolds numbers namely 13 000, 17 000,

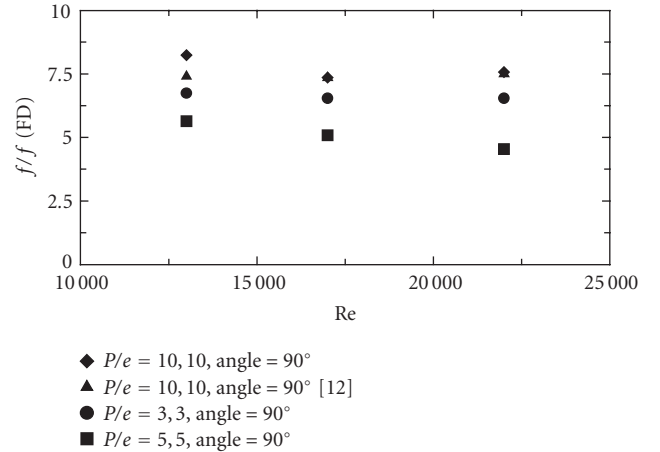


FIGURE 3: Variation of the friction factor ratio in a stationary 90° ribbed channel.

and 22 000. It can be seen that the highest friction factor ratios are observed in the case of a rib pitch-to-height ratio of 10 on both opposing surfaces. The values of the friction factor ratio for the cases  $P/e = 10, 5$  and  $P/e = 10, 8$  are comparable with that of the case  $P/e = 10, 10$ . However, the friction factor ratio is low for cases  $P/e = 3, 3$ ,  $P/e = 5, 5$ , and  $P/e = 15, 5$  when compared to that of case  $P/e = 10, 10$ . The absence of a well-defined reattachment zone for the lower rib pitch-to-height ratios accounts for the lower friction factors

observed. Similar observations have been reported in the literature for rib heights of  $e/D = 0.063$  [1] and 0.19 and 0.14 [11]. The value of the friction factor ratio for a configuration of  $90^\circ$  rib angle with a rib pitch-to-height ratio of 10 reported by Han and Chandra [12] is shown in the figure, and the comparison is seen to be very good except for the lowest Reynolds number where there is a difference of about 12%.

### 3.2. Friction factor ratio distribution in a rotating channel for a rib angle of $90^\circ$

The effect of rotation on the friction factor ratios for various orientation angles for rib pitch-to-height ratios of  $P/e = 3, 3$ ;  $P/e = 5, 5$ ;  $P/e = 10, 10$ ;  $P/e = 10, 5$ ;  $P/e = 10, 8$ ; and  $P/e = 15, 5$  is shown in Figures 4, 5, 6, 7, 8, and 9, respectively. For each Reynolds number, experiments were conducted for four rotation numbers ranging from 0.11–0.38. For each configuration, the test section was turned about its axis in steps of  $15^\circ$  from an orientation angle of  $0^\circ$  (base case with ribs on the leading and trailing surfaces) to an orientation angle of  $90^\circ$  (ribs on the top and bottom surfaces). It can be seen that at an orientation angle of  $0^\circ$  (base case), the friction factor ratio is nearly constant for all rotation numbers as compared to the corresponding stationary situation. This is observed for all rib pitch-to-height ratios studied. It can be seen that at any orientation angle other than  $0^\circ$ , the friction factor ratio increases with the increase in the rotation number. Also, the friction factor ratio increases with the increase in the orientation angle for a given rotation number. This trend is observed for all rib pitch-to-height ratios covered in this study. At an orientation angle of  $90^\circ$  (ribs on the top and bottom surfaces), the friction factor ratio is found to be the maximum during rotation.

Figure 10 shows the influence of rib pitch-to-height ratio for a rotating channel with an orientation angle of  $90^\circ$ . In general, at any orientation angle, the friction factor ratios of rib pitch-to-height ratios of 5,5 are greater compared to all other rib pitch-to-height ratios covered in this study and minimum friction factor ratios are experienced in a rib pitch-to-height ratio of 3,3 situation at any orientation angle.

Rothe and Johnston [6], in their study of backward-step flow under conditions of rotation, explained that the change in the separation lengths on the leading/trailing surfaces could be due to increased/decreased entrainment within the separation zone because of the Coriolis force-induced secondary flow structure. A similar mechanism also holds true in the present situation; the entrainment is aided by the Coriolis-force-generated secondary flow. This can be observed from the qualitative secondary flow pattern shown in Figure 2a for the  $0^\circ$ ,  $90^\circ$  and an intermediate orientation angle. The influence is the weakest for the  $0^\circ$  orientation case where the entrainment is aided on the pressure surface and hindered on the suction surface. The effect of the increased friction on the pressure surface is nullified by the reduced friction on the suction surface to give a near-constant overall friction. The reduction in the separation zone is not significant here since only the slower-moving core flow helps in the mechanism. On the contrary, the fast moving secondary fluid

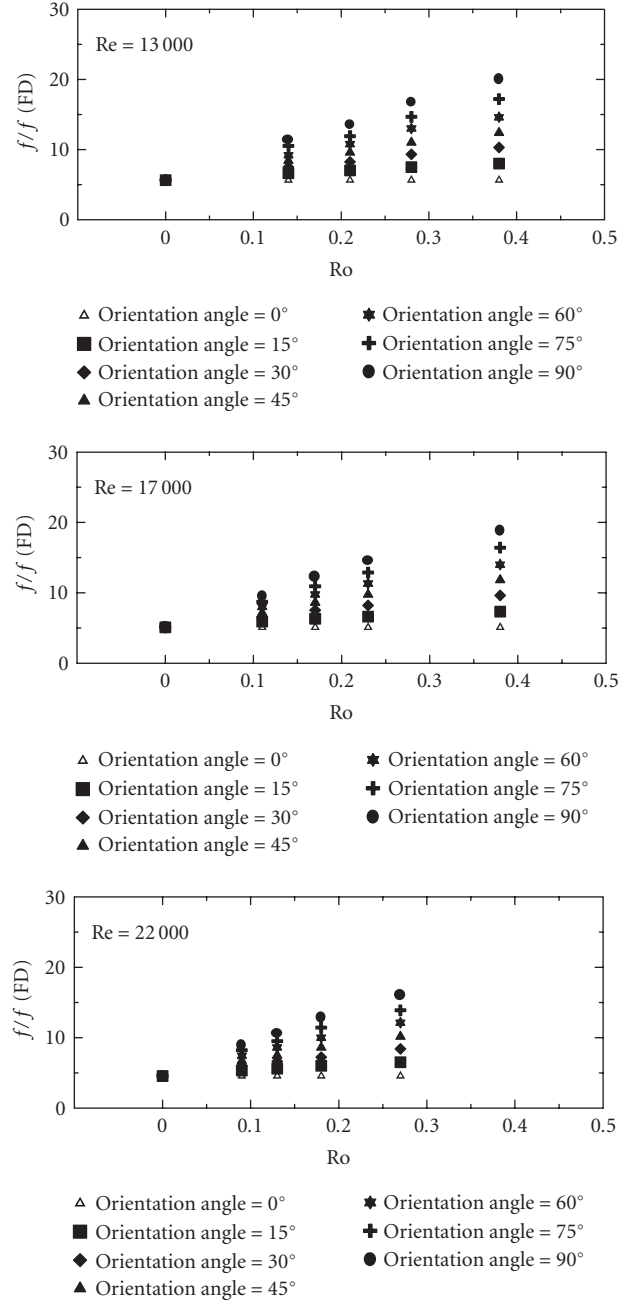


FIGURE 4: Effect of the orientation angle for  $90^\circ$  ribbed radial outward flow channel for a rib pitch-to-height ratio of 3, 3.

along the edges where the fluid moves against the Coriolis force direction (to ensure mass balance) enhances entrainment considerably and the reduction in the separation zone is considerable for the  $90^\circ$  orientation case. This is suggestive of high local velocities within the separation zone resulting in higher frictional drop. The data indeed indicates the highest friction factors for the  $90^\circ$  orientation case. The decrease in the separation zone suggests that the rib pitch-to-height ratio can be reduced from a value of 10, and still experiences distinct separation, reattachment zones. The data also reflects

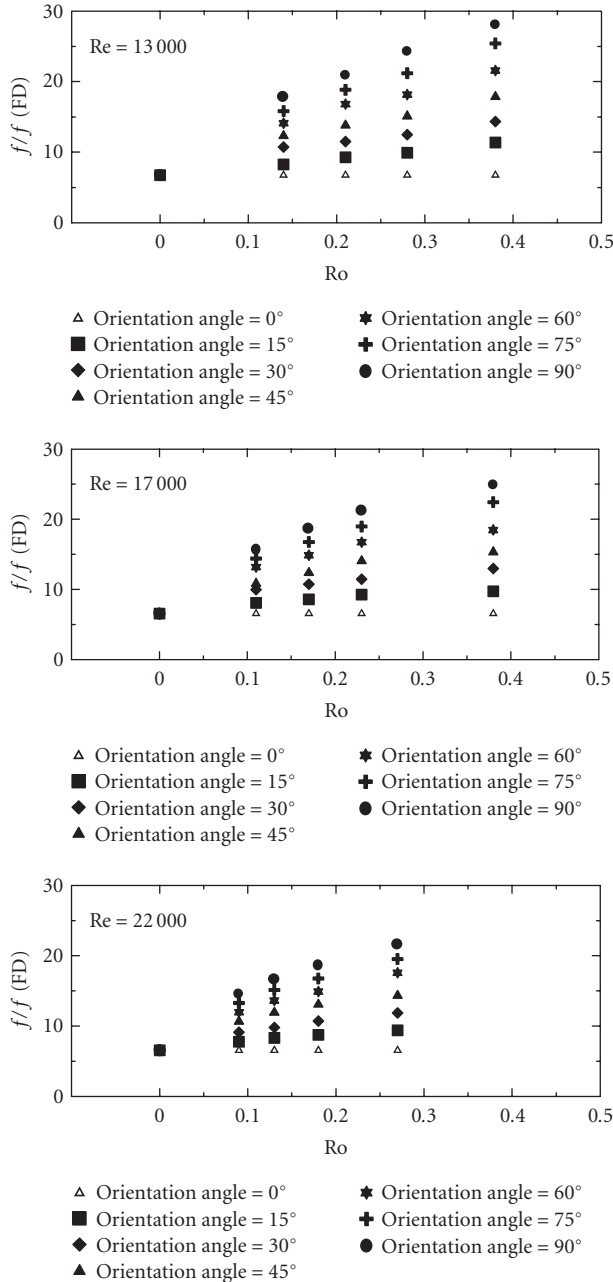


FIGURE 5: Effect of the orientation angle for  $90^\circ$  ribbed radial outward flow channel for a rib pitch-to-height ratio of 5, 5.

this in the form of the highest friction factor ratios for the rib pitch-to-height ratio of 5 on the pressure surface case. However, the data for the smaller rib pitch-to-height ratio of 3 indicates that the reduction in the separation zone is not enough anymore for producing distinct separation and reattachment zones resulting in reduced friction factors. Higher rotation numbers could possibly result in situation where the friction factor increases for a rib pitch-to-height ratios of 3 on the pressure surface. A better understanding of the flow field under conditions of rotation required to explain the

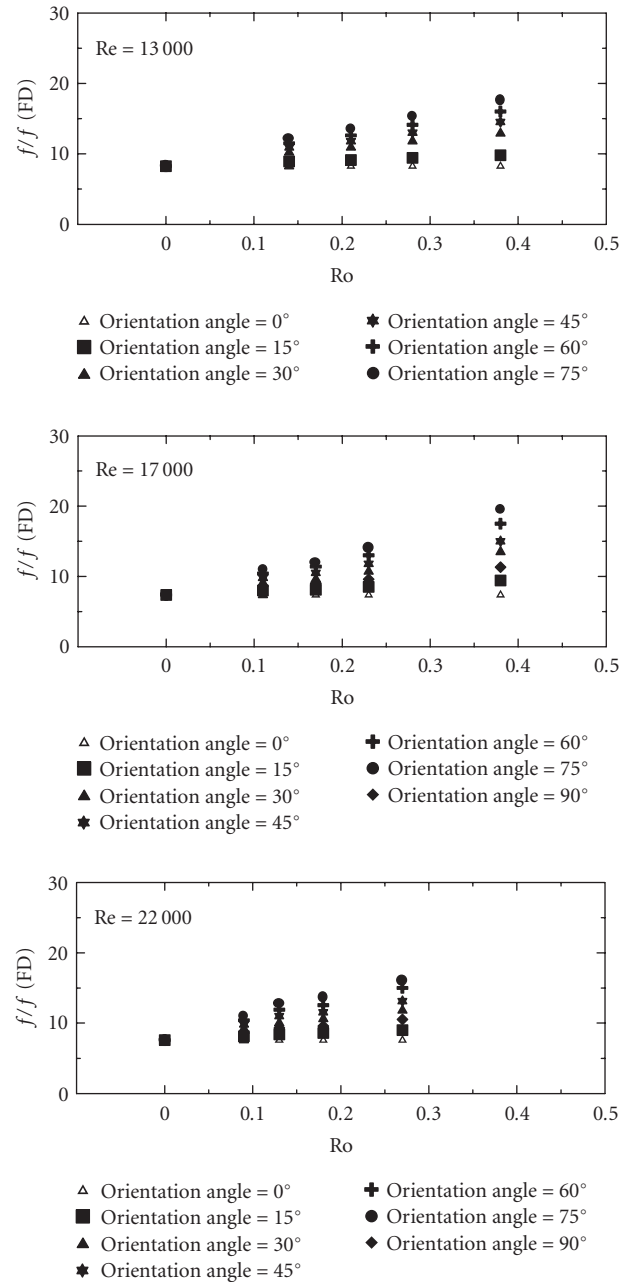


FIGURE 6: Effect of the orientation angle for  $90^\circ$  ribbed radial outward flow channel for a rib pitch-to-height ratio of 10, 10.

phenomenon completely could be obtained by more detailed pressure and velocity measurements between the ribs.

Figure 11 shows the effect of rotation on the channel with a rib angle of  $45^\circ$  and a rib pitch-to-height ratio of 10 for orientation angles of  $0^\circ$  and  $90^\circ$ . The friction factor ratio decreases with an increase in the rotation number when the ribs are placed on the leading and trailing surfaces for the zero orientation angle case. This is contrary to the  $90^\circ$  rib angle situation wherein there is no change in the friction factor ratio with rotation. The maximum decrease in the friction



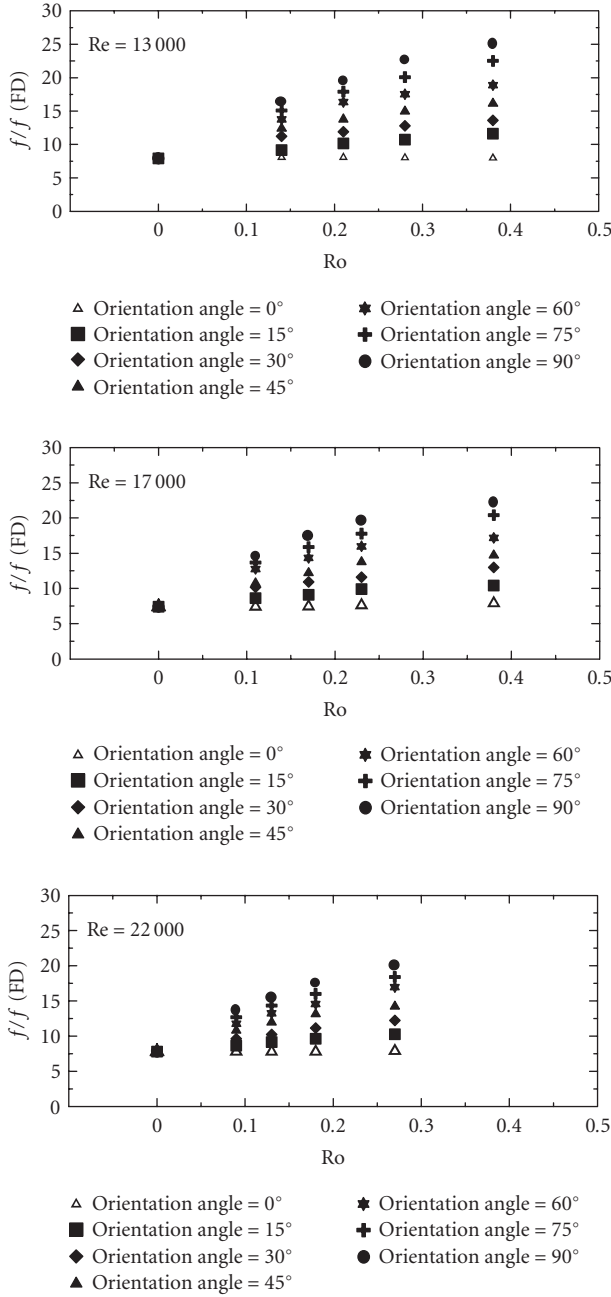


FIGURE 7: Effect of the orientation angle for  $90^\circ$  ribbed radial outward flow channel of a rib pitch-to-height ratio of 10, 5.

factor ratio is 30% at the highest rotation number of 0.38. However, at an orientation angle of  $90^\circ$ , the friction factor ratio increases only by 25%. Although a complete parametric study has not been carried out for this case, the data does suggest that the influence of rotation for the  $45^\circ$  rib case is much smaller compared to the corresponding  $90^\circ$  rib situation. This is possibly due to the rib angle-induced cross flow which interferes with the changes in the separation-reattachment behavior in the presence of rotation.

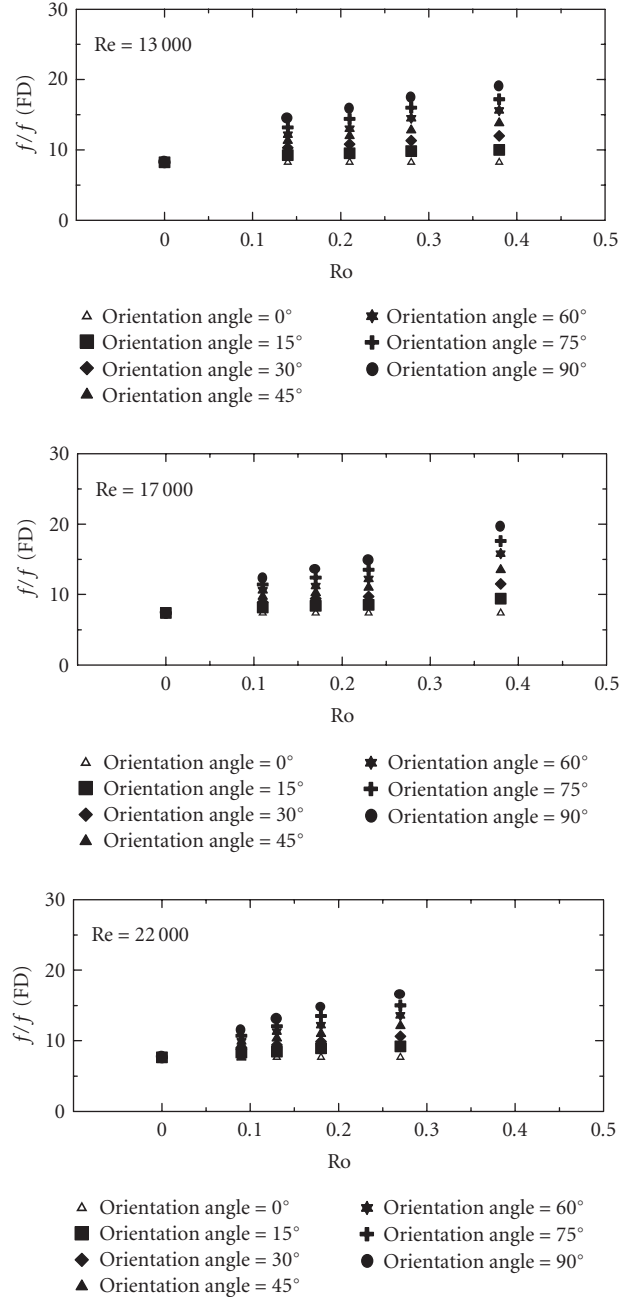


FIGURE 8: Effect of the orientation angle for  $90^\circ$  ribbed radial outward flow channel for a rib pitch-to-height ratio of 10, 8.

Figure 12 shows the variation of pressure in between two successive ribs for the  $0^\circ$  orientation case for stationary and rotating conditions. The pressure at different axial locations for the same spanwise location showing nearly identical values for the no-rotation case is expected. The small difference in slope between the first and last two axial locations is indicative of the existence of a separation zone in between the ribs. The pressure distribution in between the ribs for the situation with rotation can be noticed to be different.

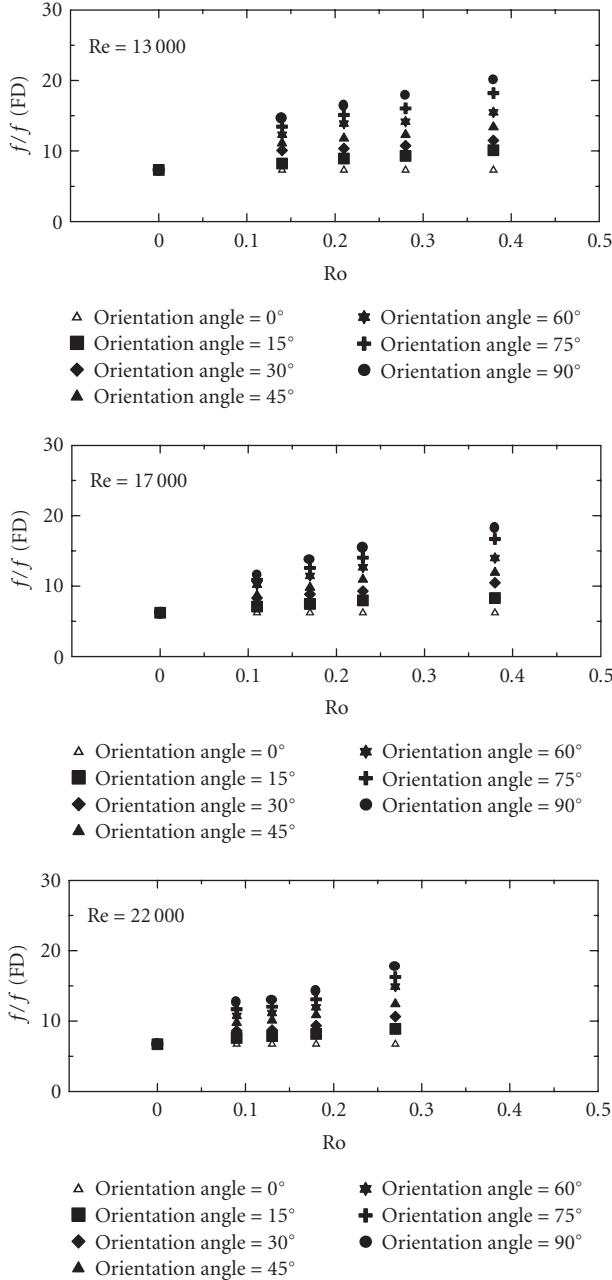


FIGURE 9: Effect of the orientation angle for 90° ribbed radial outward flow channel for a rib pitch-to-height ratio of 15, 5.

An increase in the slope of the pressure distribution in the region closer to the upstream rib, in the presence of rotation, indicates a possible shift of the reattachment point towards the upstream rib. Very little spanwise pressure variation is noticed. This is expected since the Coriolis induced cross flow is normal to the ribbed wall and therefore the effect on the wall is symmetric. Figure 13 shows the pressure distribution for an orientation angle of 90° for two rotation numbers (0.23 and 0.46). The difference between the rotation and the no-rotation case is very prominent. The slope of the curve between the first two axial locations increases

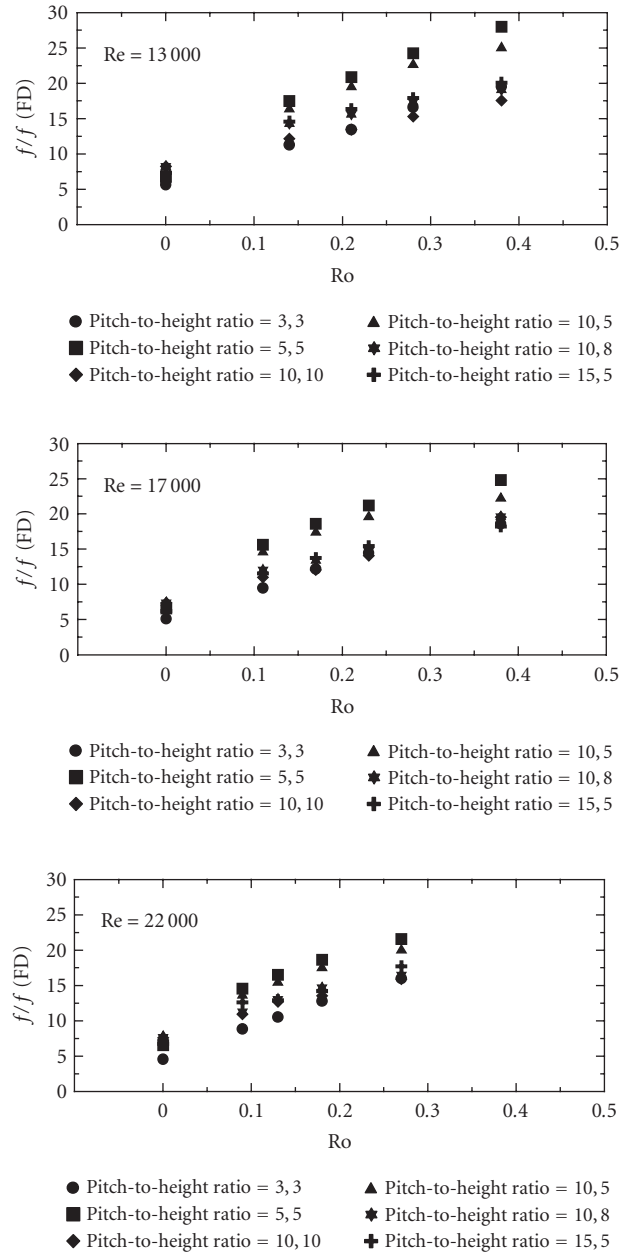


FIGURE 10: Effect of the rib pitch-to-height ratio for 90° ribbed radial outward flow channel for an orientation angle of 90°.

significantly moving along the spanwise direction from the suction to the pressure wall. This is clearly indicative of the fact that the reattachment length is small close to the pressure wall and progressively increases towards the suction wall. The reattachment zone is no longer parallel to the rib.

#### 4. CONCLUSIONS

The effect of orthogonal rotation and the channel orientation angle on the overall pressure drop in a rib-roughened radial outward flow square duct for several combinations of



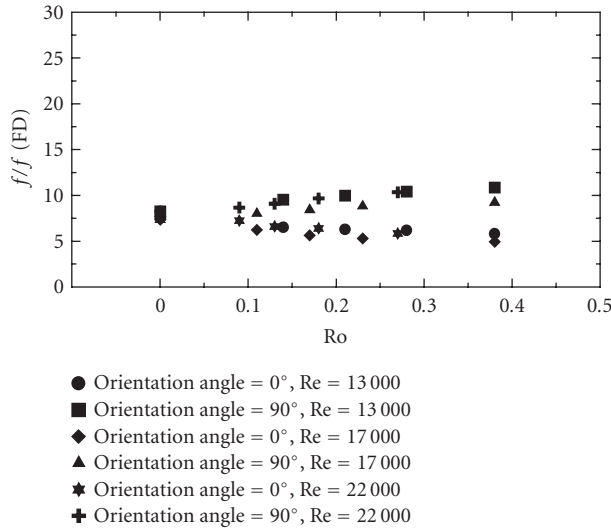


FIGURE 11: Variation of the friction factor ratio for 45° ribbed radial outward flow channel for a rib pitch-to-height ratio of 10.

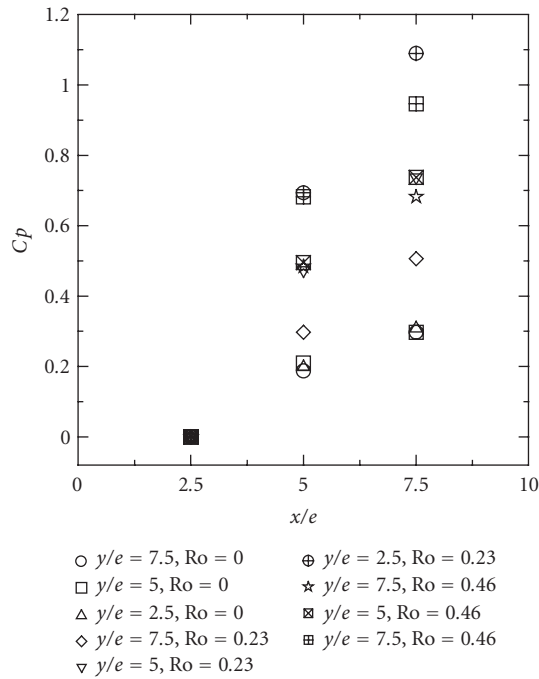


FIGURE 12: Effect of rotation number for 0° orientation at different “ $y/e$ ” locations for a Reynolds number of 18 500.

rib pitch-to-height ratios has been investigated. Rib height-to-hydraulic diameter ratio of 0.1 is maintained constant. In a stationary channel, maximum friction factor is observed for a test section with a rib pitch-to-height ratio of 10 on the opposite surfaces for a rib angle of 90°. The overall pressure drop does not change significantly for the base case under conditions of rotation. However, when the channel orientation angle varies from 0° to 90°, a monotonic increase in the overall pressure drop is observed for a constant rotation number. A continuous increase in the pressure drop

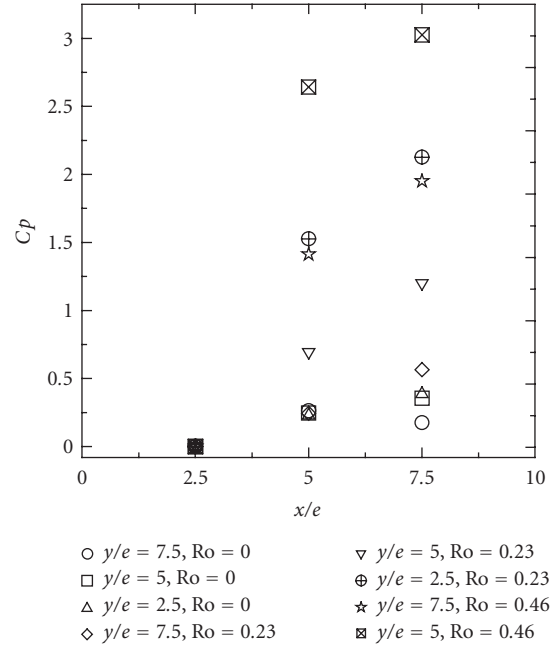


FIGURE 13: Effect of rotation number for 90° orientation at different “ $y/e$ ” locations for a Reynolds number of 18 500.

with increasing rotation number is also observed for a constant orientation angle. For a rib angle of 90°, with an orientation angle of 90°, the increase in the friction factor ratio with rotation is found to be maximum in the case of a rib pitch-to-height ratio of 5 on two opposite surfaces out of various rib pitch-to-height ratios covered in this study. The minimum friction factor ratio increase is observed in the case of a rib pitch-to-height ratio of 3 on two opposite surfaces. The local pressure drop data presented is suggestive of a significant change in the separation zone in between the ribs. It appears that the separation zone is no longer parallel to the rib surface.

For a rib angle of 45°, at an orientation angle of zero, the friction factor ratio decreases. However, at an orientation angle of 90°, the friction factor ratio increases only by 25% at the highest rotation number.

The results of the present study indicate that the rib pitch-to-height ratio and also the rib angle which may be optimum based on either maximum heat transfer or heat transfer-to-pumping power ratio consideration for stationary configuration may not be necessarily the same under conditions of rotation and changing channel orientation angle. Gas turbine internal cooling passages often use rib-roughened passages where the orientation angle may vary considerably. A single rib height-to-hydraulic diameter ratio has been studied in the present work. A detailed study on the effect of different rib height-to-hydraulic diameter ratios on the overall mechanism would be useful. Although, the increase in the friction factor indicates an increase in the heat transfer, further experiments to determine the effect of channel orientation and the variation of the rib pitch-to-height ratio on the heat transfer are required.

## REFERENCES

- [1] J. C. Han, J. S. Park, and C. K. Lei, "Heat transfer enhancement in channels with turbulence promoters," *ASME Journal of Engineering for Gas Turbines and Power*, vol. 107, pp. 628–635, 1985.
- [2] S. Okamoto, S. Seo, K. Nakaso, and I. Kawai, "Turbulent shear flow and heat transfer over the repeated two-dimensional square ribs on ground plane," *ASME Journal of Fluids Engineering*, vol. 115, pp. 631–637, 1993.
- [3] T. M. Liou, Y. Y. Wu, and Y. Chang, "LDV measurements of periodic fully developed main and secondary flows in a channel with rib-disturbed walls," *Journal of Fluids Engg.*, vol. 115, pp. 109–114, 1993.
- [4] J. C. Han and P. Zhang, "Pressure loss distribution in three pass rectangular channel with rib turbulators," *ASME Journal of Turbomachinery*, vol. 111, pp. 515–521, 1989.
- [5] M. E. Taslim and C. A. Wadsworth, "An experimental investigation of the rib surface averaged heat transfer coefficient in a rib-roughened square passage," *ASME Journal of Turbomachinery*, vol. 119, pp. 381–389, 1997.
- [6] P. H. Rothe and J. P. Johnston, "Free shear layer behavior in rotating systems," *ASME Journal of Fluids Engineering*, vol. 101, pp. 117–120, 1979.
- [7] Johnson. B. V, J. H. Wagner, G. D. Steuber, and F. C. Yeh, "Heat transfer in rotating serpentine passages with selected model orientations for smooth or skewed trip Walls," *ASME Journal of Turbomachinery*, vol. 116, pp. 738–744, 1994.
- [8] J. A. Parsons, J. Han, and Y. Zhang, "Effect of model orientation and wall heating condition on local heat transfer in a rotating two pass square channel with rib turbulators," *International Journal Heat and Mass Transfer*, vol. 38, pp. 1151–1159, 1995.
- [9] S. Dutta and J. C. Han, "Local heat transfer in rotating smooth and ribbed two-pass square channels with three channel orientations," *Journal of Heat Transfer*, vol. 118, pp. 578–584, 1996.
- [10] S. J. Kline and F. A. McClintock, "Describing uncertainties in single sample experiments," *Mech. Engrg.*, vol. 75, pp. 3–8, 1953.
- [11] Y.-J. Hong and S.-S. Hsieh, "Heat transfer and friction factor measurements in ducts with staggered and in-line ribs," *Journal of Heat Transfer*, vol. 115, pp. 58–65, 1993.
- [12] J. C. Han and P. R. Chandra, "Local heat/mass transfer and pressure drop in a two-pass rib-roughened channel for turbine airfoil cooling," Tech. Rep. 24227, NASA Lewis Research Center, Cleveland, Ohio, USA, 1987.

